JMEPEG (2004) 13:295-302
DOI: 10.1361/10599490419315

1059-9495/$19.00

Using CrAlN Multilayer Coatings to Improve Oxidation Resistance of Steel Interconnects for Solid Oxide Fuel Cell Stacks

R.J. Smith, C. Tripp, A. Knospe, C.V. Ramana, A. Kayani, Vladimir Gorokhovsky, V. Shutthanandan, and D.S. Gelles

(Submitted 22 January 2004; in revised form 6 February 2004)

The requirements of low-cost and high-temperature corrosion resistance for bipolar interconnect plates in solid oxide fuel cell stacks has directed attention to the use of metal plates with oxidation resistant coatings. The performance of steel plates with multilayer coatings, consisting of CrN for electrical conductivity and CrAlN for oxidation resistance, was investigated. The coatings were deposited using large area filtered arc deposition technology, and subsequently annealed in air for up to 25 hours at 800 °C. The composition, structure, and morphology of the coated plates were characterized using Rutherford backscattering, nuclear reaction analysis, atomic force microscopy, and transmission electron microscopy techniques. By altering the architecture of the layers within the coatings, the rate of oxidation was reduced by more than an order of magnitude. Electrical resistance was measured at room temperature.

Keywords CrAlN, coatings, corrosion resistance, interconnect, ion beam analysis

1. Introduction

Solid oxide fuel cells (SOFC) are becoming increasingly attractive as a way of converting chemical energy into electrical current by means of the electrochemical combination of hydrogen and oxygen (O) via an ion-conducting solid oxide electrolyte. The operational requirements of high ionic conductivity and good catalytic performance in the fuel cell must be balanced against the practical requirements of low-cost and high-temperature corrosion resistance for components in the fuel cell stack.[1] Of particular interest in this work is the bipolar plate serving as the current collector or interconnect between adjacent cells of the SOFC stack. The interconnect must not only retain low electrical resistivity throughout the operating lifetime of the fuel cell, but must also have good surface stability with thermal expansion and other physical properties that are compatible with the materials in the stack.[2] Doped $LaCrO_3$ plates have worked well for cells operating at 1000 °C but suffer from high cost as well as difficulties in fabrication. The recent trend toward lower operating temperatures (500–750 °C) may enable the use of more cost-effective materials for the current collector. A thorough evaluation of several heat-resistant alloys with a variety of compositions led to the conclusion that it would be difficult for most traditional alloys to meet the materials requirements of long-term operation above 700 °C.[3] Alloys of body-centered-cubic (bcc) ferritic stainless steels appear to have thermal expansion coefficients that are well matched to other components in the stack but do not have a sufficiently high electrical conductivity for the desired operating lifetime. The authors conclude that for improved oxidation resistance and electrical conductivity either new alloys will need to be developed, or surface engineering of existing alloys will be required.[3] Among candidate materials in the former category is Crofer22 APU, an Fe–Cr-based ferritic stainless steel with additional manganese, available from ThyssenKrupp VDM (Werdohl, Germany). The present work falls into the latter category of surface engineering, namely, the use of coatings to improve oxidation resistance while maintaining acceptably low resistivity values. Related research on surface engineering includes the use of conducting oxide coatings and thermal nitriding.[4] The use of coatings for this application brings with it an additional set of problems, namely, guaranteeing the integrity of the coating with respect to adhesion, wear resistance, and detrimental effects associated with interdiffusion between coating and substrate material. On the other hand, using coatings may enable the use of inexpensive alloys that would otherwise be ruled out due to their poor oxidation resistance.

The use of coatings to improve oxidation resistance on metal alloys has been known for many years. We selected the Cr–Al–N system for study because it not only offers oxidation resistance at temperatures up to 900 °C[5,6] but also provides wear resistance typical of many metal nitrides.[7] Furthermore, a multilayer structure consisting of AlN and CrN layers was used with the goal to study the affect of individual layer thickness on oxidation kinetics for the coating. It is known that

This paper was presented at the Fuel Cells: Materials, Processing, and Manufacturing Technologies Symposium sponsored by the Energy/Utilities Industrial Sector & Ground Transportation Industrial Sector and the Specialty Materials Critical Technologies Sector at the ASM International Materials Solutions Conference, October 13-15, 2003, in Pittsburgh, PA. The symposium was organized by P. Singh, Pacific Northwest National Laboratory, S.C. Deevi, Philip Morris USA, T. Armstrong, Oak Ridge National Laboratory, and T. Dubois, U.S. Army CECOM.

R.J. Smith, C. Tripp, A. Knospe, C.V. Ramana, and **A. Kayani,** Physics Department, Montana State University, Bozeman, MT 59717; **Vladimir Gorokhovsky,** Arcomac Surface Engineering, Bozeman, MT 59715; and **V. Shutthanandan** and **D.S. Gelles,** Pacific Northwest National Laboratory, Richland, WA 99352. Contact e-mail: smith@physics.montana.edu.

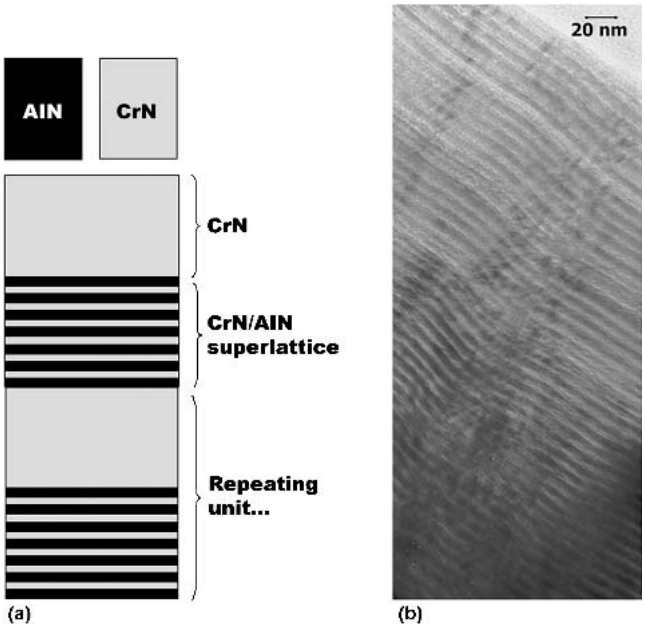

Fig. 1 **(a)** Schematic drawing of the multilayer structure of the LAFAD coatings consisting of repeated sections of CrN and a CrAlN superlattice. **(b)** TEM image of the multilayer coating showing the CrN (dark bands) and CrAlN superlattice (light bands). The bar in the upper right represents a distance of 20 nm.

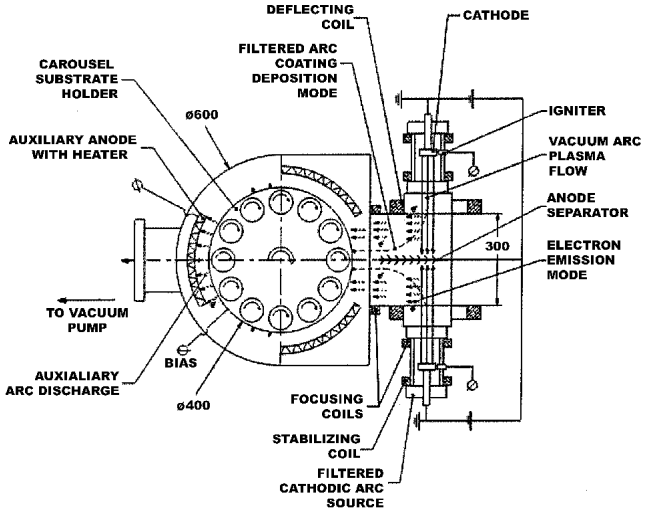

Fig. 2 Schematic drawing of the LAFAD deposition chamber (top view) showing the dual arc sources and the sample carousel

exposing CrN to O at elevated temperatures leads eventually to loss of nitrogen and formation of Cr_2O_3,[8] a semiconductor with sufficiently low resistivity for the interconnect application at an operating temperature of 800 °C.[9] The oxidation of AlN leads to the formation of Al_2O_3 with unacceptably low conductivity for the interconnect, yet alumina is known to be a good oxidation-resistant barrier. Our approach was to consider a variety of multilayer structures with nanometer-thick layers of CrN alternating with a superlattice layer comprised of several sub-nanometer thick layers of AlN and CrN [Fig. 1(a)]. It is expected that the thin alumina layers will be sufficiently discontinuous to have electron conduction pathways through the chromia, or if continuous, be sufficiently thin to have significant electron current via tunneling. These coatings were deposited on stainless steel disks using dual large area, filtered arc sources.[10] Sample characterization included electron microscopy and ion beam analysis for structure and composition of the coating, atomic force microscopy (AFM) for surface roughness, and area specific resistance (ASR) for electrical conductivity. The films were annealed at 800 °C in air for up to 25 h, followed by characterization of composition and surface roughness.

2. Experimental Procedure

For this initial study circular disks of 304 and 440A stainless steel, 19.05 mm (0.75 in.) diameter and 3.175 mm (0.125 in.) thick, were chosen as substrates. The disks were mechanically polished on 1500 grit SiC paper. The multilayer coatings were deposited at Arcomac Surface Engineering using the Large-Area Filter Arc Deposition (LAFAD) technology with the patented rectangular Large-Area Filtered Arc Source (LAFAS, Acromac Surface Engineering, Bozeman, MT). This approach overcomes the limitations of conventional filter designs.[10] LAFAS uses a rectangular plasma-guide chamber with two rectangular deflecting coils installed on the opposite sides, as shown in Fig. 2. In this design, two primary cathodic arc sources utilizing Cr and Al targets are placed opposite each other on the sidewalls of the plasma-guide chamber, surrounded by rectangular deflecting coils, and separated by an anodic baffle plate. The LAFAS vapor plasma source uses a superimposed deflecting magnetic field to turn the metal ion flow 90° toward the deposition chamber and substrates. More massive droplets of material from the source follow straighter trajectories and are captured on baffles, resulting in droplet-free coatings. A set of scanning magnetic coils allows the ion plasma jet to be swept in the vertical direction so as to cover theoretically unlimited large surface areas. At the same time, the arc column is well confined by a magnetic field in the horizontal direction, providing enhanced suppression of the turbulent plasma diffusion, leading to a significant increase in the metal vapor ion yield. By manipulating the arc plasma jets using strategically placed scanning magnetic coils and auxiliary anodes, this novel design creates a "plasma-immersion" environment in the coating chamber. This technique allows the plasma flux from different cathodes in a multi-cathode chamber to be uniformly mixed and completely envelop complex parts. The use of auxiliary anodes in conjunction with the filtered arc sources permits extraction of a significant electron current from the arc source, which provides a highly conductive ionized gas even without the metal plasma.[10]

The substrates were mounted on rotating pedestals distributed about the outer rim of a rotating carousel in the chamber. With both the pedestals and carousel rotating, referred to as double rotation (DR), both sides of the disks were exposed to the arc sources several times per revolution of the platform. With the pedestal rotation disabled, referred to as single rotation (SR), the target rotated with the carousel in the chamber. The single rotation process placed one surface of the disks in

Table 1 Structure Parameters of CrAlN Coatings on 304 Stainless Steels

Sample	*m*, s	*n*, s	*p*, reps	Description
026	40	20	60	60 *m* SR
028	40	20	60	60 *m* DR
036	…	4 h	…	superlattice

The notation used to describe the structures is {(CrN)*m*/(CrN/AlN)*n*}*p* with *m* and *n* being the deposition time in seconds except as noted, and *p* being the number of repetitions for the multilayer structure.

front of the respective Cr or Al sources for longer times, once per platform revolution, resulting in thicker individual layers. The multilayer structure shown schematically in Fig. 1(a) was achieved by periodically blocking the Al source, allowing for longer deposition periods of CrN only. Thickness of the individual layers in the superlattice substructure of the coating was determined by the rotation speed of the carousel (~10 rpm) in the chamber, and estimated to be about 0.4 nm. The substrate temperature during deposition was about 500 °C. The substrates were first cleaned in an Ar ion plasma at 8×10^{-2} Pa for 20 min followed by 2 min of high voltage Cr ion etching in argon (2×10^{-2} Pa). The Cr and Al ions were deposited in N at 4×10^{-2} Pa with a 50 V bias voltage at 40 kHz using a low-frequency bias power supply. With these conditions the overall deposition rate was approximately 0.5 μm/h for single rotation with both the Cr and Al sources running. Overall coating thickness varied, depending on total deposition time and rotation mode. The coatings considered here are listed in Table I. To describe the coating structure, we use the notation [(CrN)*m*/(CrN/AlN)*n*]*p*, with *m* and *n* being the deposition time in seconds, except as noted in Table I, and *p* being the number of repetitions for the multilayer structure. The deposition rate (nm/s) with both sources on (superlattice) is about twice that with the AlN source blocked, so choosing the time *m* to be twice the value of *n* results in roughly equal layer thickness for the multilayer structure; i.e., 40 s of CrN followed by 20 s of CrN/AlN superlattice is estimated to give layers that are each about 3.8 nm thick. Individual layers in the superlattice were estimated to be about 0.6 nm thick for single rotation and 0.3 nm for double rotation. The transmission electron microscope (TEM) image of Fig. 1(b) shows a cross section of one of the coatings (026 in Table I) prior to oxidation treatment. The light-colored bands correspond to the lower density CrN/AlN superlattice, and the dark bands are the CrN layers. The resolution is not sufficient to see the individual layers of the superlattice within the light band. We believe the wavy character of the bands can be attributed to polishing of the substrate prior to deposition. In the double rotation mode, the thickness of each layer is reduced by a factor of about 1.6 because both sides of the sample are coated in the same deposition time.

Oxidation of the samples was carried out using a standard tube furnace operated horizontally in air, with no additional fixtures to control humidity or flow rate. Samples were mounted vertically in a ceramic cassette at the center of the horizontal furnace tube. The oven temperature was controlled electronically with a 30 min rise time to 800 °C. Soak times were incremented to give total oxidation periods of 1, 4, 9, 16, and 25 h. After each increment of oxidation time, the oven was cooled over a period of 30 min. The samples were removed and placed in the vacuum chamber for ion beam analysis. Surface microscopy was performed prior to oxidation and at the end of the 25 h oxidation period. Electrical measurements consisted of ASR at room temperature using Al foil electrodes covering the entire disk and a stack configuration under pressure. Typically, a voltage on the order of 1–2 V was required to initiate current flow for the more heavily oxidized samples, presumably to overcome the thin insulating layers that formed on the surface of the coatings. Measurements of ASR using standard procedures with Pt paste electrodes [3] on pre-oxidized samples and for extended periods of time are still in progress.

3. Results and Discussion

Figure 3 shows AFM images recorded in tapping mode after deposition of the coatings (left column), and again after 25 h of oxidation at 800 °C in air (right column) for samples 026 (panel a and b), 028 (panel c and d), and 036 (panel e and f). The lateral width for each image is 3 μm, and the image locations are not the same for a given sample. It can be seen that the superlattice coating (036) is by far the smoothest on a submicron scale, although the coating has considerable rms roughness (82.4 nm). In contrast, sample 026 has a root-mean-square (rms) roughness of only 11.1 nm, although it appears rougher on a submicron scale. The rms roughness for sample 028 is 8.89 nm before oxidation. After oxidation, the measured rms roughness for sample 026 (SR) is not changed although the surface appears to have a more fine-grain texture. Sample 036 (superlattice) has decreased in overall roughness following oxidation although there appears to be an increase in roughness at the submicron scale. The most noticeable change following oxidation occurs for sample 028 (DR). The roughness increases by an order of magnitude to 82 nm, and the surface consists of large nodules. Based on results from the TEM and Rutherford backscattering spectra (RBS) analysis, these nodules probably correspond to clusters of Fe oxide. Diffusion of Fe to the surface of this coating is observed in both RBS and TEM, and may be an indication of cracking or other forms of degradation of the coating following the 25 h oxidation exposure at 800 °C.

Ion beam analysis of the samples was performed using the 3 MV tandem accelerator at the Environmental Molecular Sciences Laboratory (EMSL) at Pacific Northwest National Laboratory (PNNL) in Richland, WA. RBS data were recorded using a 2.0 MeV beam of He^+ ions with a 60° angle of incidence measured from the sample normal. Backscattered ions were collected using a silicon surface barrier detector at a scattering angle of 160° with an exit angle of 40° from the sample normal. This geometry enhanced the depth resolution of the RBS measurements. Spectra were collected after total oxidation periods of 1, 4, 9, 16, and 25 h at 800 °C. The samples were removed from the oven for ion beam analysis and were thus subjected to some thermal cycling that might have adversely affected the coatings. Composition profiles were determined by comparing SIMNRA computer simulations of the spectra with the original data.[11] Since the depth resolution of RBS with these beam parameters and detectors is greater than 15 nm, no attempt was made to simulate individual layers in the coating, but rather the

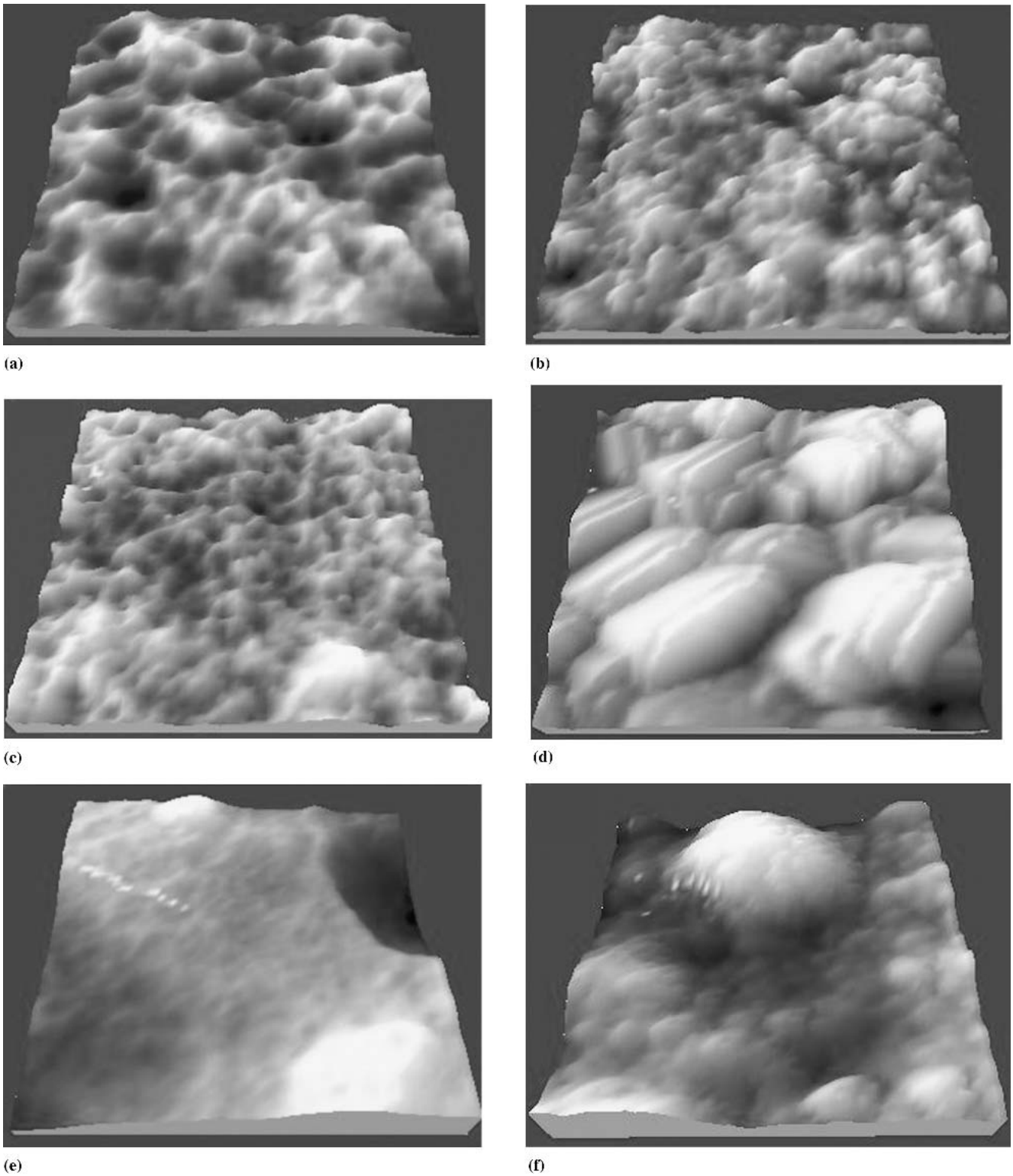

Fig. 3 AFM images of three multilayer coatings before (left column) and after (right column) oxidation in air at 800 °C for 25 h. Each image has a lateral size of 300 micrometers. Panels **(a)** and **(b)** are for the single rotation coating (026); panels **(c)** and **(d)** for the double rotation coating (028); panels **(e)** and **(f)** for the thick superlattice (036).

sample was divided into the minimum number of layers needed to give a reasonable fit to the spectrum. The composition profiles determined in this way are shown in Fig. 4 for samples 026 (a and b), 028 (c and d), and 036 (e and f) before and after 4 h of oxidation at 800 °C. The depth scale (10^{15} atoms/cm^2) is characteristic of the RBS measurement, which determines only

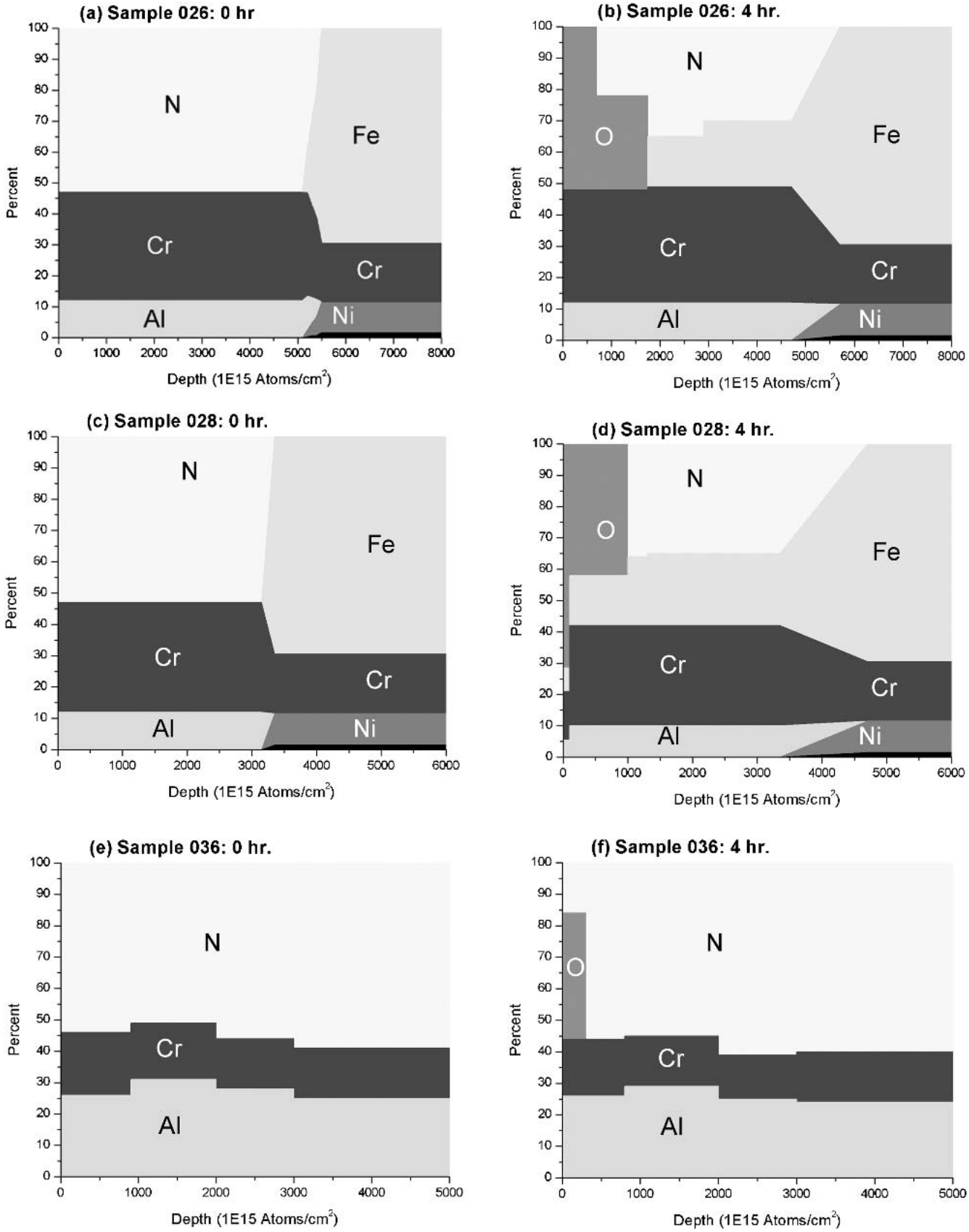

Fig. 4 Profiles of concentration versus depth are shown for the three samples discussed in the text, before (left column) and after (right column) oxidation in air at 800 °C for 1 h. The profiles are determined by fitting model spectra (SIMNRA) to the measured RBS. Relative concentrations are normalized to add to 100%, and the various concentration regions are labeled with the elemental symbols.

the number of target atoms per square centimeter visible to the analysis beam. If the sample density is known, this scale is readily converted to a linear depth scale. Since independent knowledge of the density in the coating was unknown, the average atomic density of CrN and AlN (1.183×10^{23} at/cm^3) was used to determine that approximately 1000×10^{15} atoms/cm^2 correspond to an 85 nm depth. From Fig. 4 the coating in sample 026 (SR) was determined to be about 448 nm and the thinner coating for sample 028 (DR) about 275 nm. The superlattice sample 036 was considerably thicker. Its thickness from the deposition time of 4 h is estimated to be about 1.73 μm. The TEM image of Fig. 1(b) gives a thickness of 462 nm for sample 026 (SR), which is in excellent agreement with the RBS measurement. The average composition of the two multilayer coatings analyzed in Fig. 3 is Al(0.12)Cr(0.35)N(0.53). For the superlattice coating (036), the average composition is Al(0.26)Cr(0.22)N(0.52). The superlattice composition is different from the multilayer because the Al source is on continuously.

The three coatings analyzed here behave very differently when subjected to the high-temperature oxidizing environment. The thinner sublayers of sample 028 (DR) are susceptible to Fe diffusion from the substrate to the coating surface after only 4 h in the oven. An oxide scale forms on the surface as well, and may be the material seen as clusters in the AFM image in Fig. 3(d). The thicker sublayers of sample 026 (SR) appear to slow down the Fe diffusion from the substrate. Figure 4(b) suggests that the development of an oxide on the surface of the coating effectively stops the outward diffusion of Fe from the substrate. The superlattice coating analyzed in Fig. 4(f) on the other hand appears to have oxidized far less than the two multilayer coatings. No Fe diffusion is seen in this profile, but the coating was considerably thicker and there may not have been sufficient time for the Fe to diffuse out into the coating after only 4 h After 25 h of annealing the superlattice sample (036) at 800 °C, there is still no sign of significant Fe diffusion into the coating. One possible conclusion from the RBS measurements is that the superlattice structure is an effective diffusion barrier for Fe moving from the substrate into the coating. Negligible Fe is detected for the thick superlattice (036) even after 25 h of annealing, while the two multilayer structures show significant diffusion of Fe into the coating already after only 1 h at the high temperature. Diffusion of Fe in sample 026 (SR), with the thicker superlattice layers (~3.8 nm), is somewhat slower than for sample 028 (DR), which has the thinner superlattice layers (~2.4 nm). The oxide growth rate also appears to be slowest for the thick superlattice. The final thickness of the oxide after 25 h for sample 026 (SR) is somewhat greater than that for sample 028 (DR), but this may be related to the more rapid outdiffusion of Fe in the latter, and the apparent slowing down of oxide growth when the two diffusing species meet. We have most likely oversimplified the mechanisms of oxide formation for the multilayer since loss of N from the CrN as it transforms to Cr_2N at high temperature may be playing a role in the oxidation of the multilayer.[8,12] Results similar to these were reported for high-temperature oxidation of CrN films on steel.[13] In those experiments, x-ray photoelectron spectroscopy (XPS) depth profiles show that in addition to the transformation from CrN to Cr_2O_3, FeO is forming at the surface as Fe diffuses from the steel substrate out through the CrN coating. Enhanced diffusion can occur at the higher temperatures where the mismatch in the thermal expansion coefficients between substrate and coating result in film stress and loss of adhesion at the coating/substrate interface. Images from TEM analysis suggest that there may be cracking in these coatings, and this may allow for the diffusion of Fe into the coating. It appears that the presence of the superlattice in our multilayer coatings reduces the amount of Fe diffusion from the substrate.

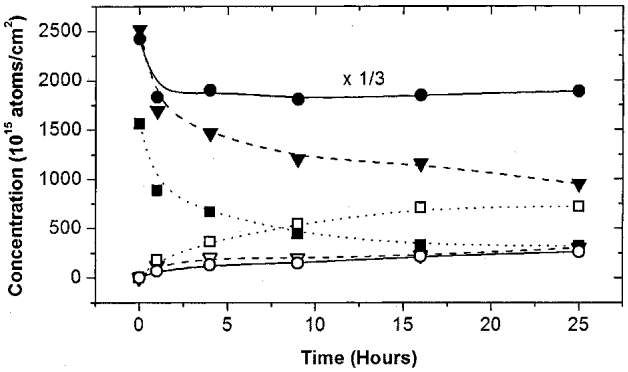

Fig. 5 Plots of total O (open symbols) and total nitrogen (solid symbols) concentrations in the multilayer coatings as a function of annealing time at 800 °C in air. The concentrations were determined using nuclear reaction analysis with a 1.0 MeV deuterium beam as described in the text. Curves are shown for sample 026 (triangles), 028 (squares), and the superlattice (circles). The N curve for the thick superlattice is reduced by a factor of three.

RBS is particularly useful for obtaining concentration depth profiles for the heavier elements in the coating but is somewhat limited in detecting the light elements such as O and N due to the quadratic dependence of the Rutherford cross section on the atomic number of the target atom. Nuclear reaction analysis (NRA) can be quite useful in this case because the spectral peaks typically sit on very low or zero background signal.[14] A limitation for NRA is that the reaction cross sections are generally known only for a few selected scattering angles and thus may need to be measured using standard thin films of known stoichiometry. For the present measurements a beam of 1.0 MeV deuterium ions (d^+) was incident on the samples at an angle of 60° from the normal. Reaction products were detected at a scattering angle of 170°, i.e., 50° from the sample normal. A thin aluminized Mylar film covered the detector to stop backscattered deuterium ions, allowing only the more energetic reaction products to enter the detector. The detected particles for these measurements were protons from the $^{14}N(d,p)^{15}N$ and $^{16}O(d,p)^{17}O$ reactions. The reaction cross sections for the experimental geometry were determined in a separate experiment using commercially prepared films of Si_3N_4 and SiO_2 with known thickness. Peak areas from the measured yields were converted to N or O concentrations. Since the depth resolution for these particular reactions is not nearly as good as that for the RBS measurements, our purpose was to determine the total N and O concentrations in the coatings as a function of annealing. These total concentrations were then compared with the total concentrations determined from the RBS measurements. The set of target composition profile parameters was adjusted until a single set of parameters could be used to accurately simulate both the RBS and NRA measurements using

the SIMNRA program. The results are shown in Fig. 5 for the three samples listed in Table 1. The measurements show a decrease in total N content (solid symbols) and a gradual increase of O (open symbols) as a function of annealing time. In every case, there is a rapid decrease in N content following the initial 1 h heat treatment, attributed to the transformation of CrN to Cr_2N.[8,12] A more gradual loss of N during subsequent annealing is attributed to the transformation of Cr_2N to Cr_2O_3. The total N content varies from sample to sample due to the different multilayer structures and coating thickness. The superlattice has a much higher N concentration due to the greater coating thickness (~2.5 μm). The observed rate of oxide growth is greatest for sample 028, with the thinner superlattice layers, and more than a factor of two smaller for samples 026 (thicker superlattice layers) and 036 (thick superlattice with no CrN layers). These results are consistent with those discussed above for RBS, and show clearly the trends in N and O concentrations as a function of annealing time at 800 °C.

The effectiveness of the coatings can be easily seen if we compare the results of Fig. 5 to those for a blank steel disk with no coating. The NRA measurements of total O content for the blank disk were stopped after 10 h at 800 °C due to excessive spalling of the oxide scale. At that point, the total O concentration remaining on the disk was at a level of 6400×10^{15} atoms/cm^2, approximately a factor of 40 greater than that shown for samples 026 and 036 in Fig. 5. In the future the results of oxide growth for coated steel disks will be compared with those from several steel alloys specifically designed for oxidation resistance, such as the Crofer22 APU.

Finally, a quantitative means for comparing the oxidation resistance of the samples analyzed in these experiments is provided. The results from ion beam analysis are quantitative and can be used to show either total O content or oxide thickness as a function of time, as plotted in Fig. 5. The former is more straightforward to obtain since it does not depend on the oxide stoichiometry, which might change with depth. Since the kinetics of oxide growth exhibit a square-root dependence on time for many metal-oxide systems, a parabolic curve of the form $[(\text{Yield})^2 = C \times t]$ was used to describe the oxide growth data in Fig. 4. The units of the proportionality constant in this case, with time given in hours, are $[(10^{15}\ \text{at/cm}^2)^2/\text{h}]$, or approximately [(monolayer)^2/h], since the area density of atoms on a typical metal surface is about 1 to 2×10^{15} at/cm^2. The results of the curve fit exercise are shown in Table 2 and clearly demonstrate the effectiveness of the superlattice in reducing the rate of oxide growth. Missing in this discussion is the electrical characterization of the steel disks with the coatings. Measurements of ASR at temperatures up to 800 °C for these coated steel disks are still in progress, but preliminary results for a single-rotation coating identical to that of sample 026, but on a 440A steel disk, give a value of about 10 mΩ cm^2 after 800 h oxidation at 800 °C. This value is quite close to the values reported for several advanced alloys being considered for interconnect applications.[3]

In summary, early results have been reported for the high-temperature oxidation resistance of 304 stainless steel alloys with a multilayer coating of CrN and AlN. Ion beam analysis shows that oxidation rates can be greatly reduced with these coatings, and point to a superlattice structure with subnanometer layer thickness as having good performance for periods up to 25 h at 800 °C in air. Future measurements will extend the annealing time to better simulate the interconnect application in a solid oxide fuel cell.

Table 2 Rate Constants for Oxidation of CrAlN Coatings on 304 Stainless Steels

Sample	C $(10^{15}\ \text{at/cm}^2)^2$ h	Approximate SL Thickness
026	3700	60 *m* SR (3.8 nm)
028	24 634	60 *m* DR (2.4 nm)
036	2801	Superlattice (1.73 μm)

Acknowledgments

We acknowledge the technical assistance of N. Williams and J. Getty at Montana State University, and O. Popov and D. Jones at Arcomac for deposition of coatings. AFM was performed at Image and Chemical Analysis Lab (ICAL), located at Montana State University. P. Gannon and Prof. M. Deibert, Chemical Engineering Dept., Montana State University provided preliminary ASR results. Ion beam analysis was performed at the Environmental and Molecular Sciences Laboratory (EMSL), a national scientific user facility located at PNNL and supported by the United States Department of Energy's (DOE) Office of Biological and Environmental Research. Work at PNNL (EMSL) supported through Office of Biological and Environmental Research (OBER) (DOE). Pacific Northwest National Laboratory (PNNL) is a multi-program national laboratory operated for the U.S. DOE by Battelle Memorial Institute under contract No. DE-AC06-76RLO 1830. Work at MSU was supported through the High-Temperature Electrochemisty Center (HiTEC), jointly supported by a Department of Interior (DOI) and DOE subcontract from PNNL, No. 3917(413060-A). Work was also supported by a joint DOI and DOE subcontract from PNNL, No. 3917(413060-A).

References

1. B.C.H. Steele and A. Heinzel: "Materials for Fuel-Cell Technologies," *Nature*, 2001, *414,* pp. 345-52.
2. Z.G. Yang, J.W. Stevenson, and P. Singh: "Solid Oxide Fuel Cells," *Adv. Mater. Proc.*, 2003, *161*(6), pp. 34-37.
3. Z. Yang, K.S. Weil, D.M. Paxton, and J.W. Stevenson: "Selection and Evaluation of Heat-Resistant Alloys for SOFC Interconnect Applications," *J. Electrochem. Soc.,* 2003, *150*(9), pp. A1188-A1201.
4. Z.G. Yang, M.S. Walker, and J.W. Stevenson: "Application of Conductive Oxide Overlay Coatings on Ferritic Stainless Steel SOFC Interconnects for Decreased Electrical Resistance," Program of Materials Solutions 2003, 13-15 October 2003, Pittsburgh, PA; P.F. Tortorelli, M.P. Brady, K.L. More, L.R. Walker, I. Paulauskas, and R. Buchanan, "Alloy and Process Development of Thermally Nitrided Metallic Bipolar Plates for Proton Exchange Membrane Fuel Cells," Program of Materials Solutions 2003, 13-15 October 2003, Pittsburgh, PA.
5. M. Kawate, A.K. Hashimoto, and T. Suzuki: "Oxidation Resistance of $Cr_{1-x}Al_xN$ and $Ti_{1-x}Al_xN$ Films," *Surf. Coat. Technol.*, 2003, *165,* pp. 163-67.
6. O. Banakh, P.E. Schmid, R. Sanjines, and F. Levy: "High-Temperature Oxidation Resistance of $Cr_{1-x}Al_xN$ Thin Films Deposited by Reactive Magnetron Sputtering," *Surf. Coat. Technol.,* 2003, *163-164,* pp. 57-61.
7. S. PalDey and S.C. Deevi: "Single Layer and Multilayer Wear Resis-

tant Coatings of (Ti,Al)N: A Review," *Mater. Sci. Eng.*, 2003, *A342,* pp. 58-79.
8. F-H. Lu, H-Y. Chen, and C-H. Hung: "Degradation of CrN Films at High Temperature Under Controlled Atmosphere," *J.Vac. Sci. Technol. A*, 2003, *21*(3), pp. 671-75.
9. K. Huang, P.Y. Hou, and J.B. Goodenough: "Reduced Area Specific Resistance for Iron-Based Metallic Interconnects by Surface Oxide Coatings," *Mater. Res. Bull.,* 2001, *36,* pp. 81-95.
10. V.I. Gorokhovsky, R. Bhattacharya, and D. G. Bhat: "Characterization of Large Area Filtered Arc Deposition Technology: Part I – Plasma Processing Parameters," *Surf. Coat. Technol.,* 2001, *140,* pp. 82-92; V.I. Gorokhovsky, D.G. Bhat R. Shivpuri, K. Kulkarni, R. Bhattacharya, and A.K. Rai: "Characterization of Large Area Filtered Arc Deposition Technology: Part II: – Coating Properties and Applications," *Surf. Coat. Technol.* 2001, *140,* pp. 215-24.
11. M. Mayer, *SIMNRA User's Guide,* Technical Report IPP 9/113, Max-Planck-Institut fur Plasmaphysik, Garching, Germany, 1997.
12. H-Y. Chen and F-H. Lu: "Phase Transformation in Chromium Nitride Films," *J.Vac. Sci. Technol. A*, 2003, *21*(3), pp. 695-700.
13. I. Milosev, J.M Abels, H-H. Strehblow, B. Navinsek, and M. Metikos-Hukovic: "High Temperature Oxidation of Thin CrN Coatings Deposited on Steel," *J. Vac. Sci. Technol. A,* 1996, *14*(4), pp. 2527-34.
14. Anon., *Handbook of Modern Ion Beam Materials Analysis,* J.R. Tesmer and M. Nastasi, ed., Materials Research Society, Pittsburgh, PA, 1995.